Proceedings of the 1997 IEEE
International Conference on Robotics and Automation
Albuquerque, New Mexico - April 1997

Estimation of Track-soil Interactions for Autonomous Tracked Vehicles

Anh Tuan Le, David.C. Rye and Hugh.F. Durrant-Whyte

Department of Mechanical & Mechatronic Enginering
The University of Sydney 2006 NSW, Australia.
e-mail: {tuan|rye|hugh}@mech.eng.usyd.edu.au

Abstract

Real time estimation of soil parameters is essential in achieving precise, robust autonomous guidance and control of a tracked vehicle. The paper shows that the slip of the tracks over the terrain can be identified from trajectory data using an extended Kalman filter. The use of a suitable soil model can then allow key soil parameters to be estimated as the vehicle passes over the soil. Knowledge of the soil parameters may in turn be used to allow reference trajectories and control algorithms to be adjusted to suit the soil conditions.

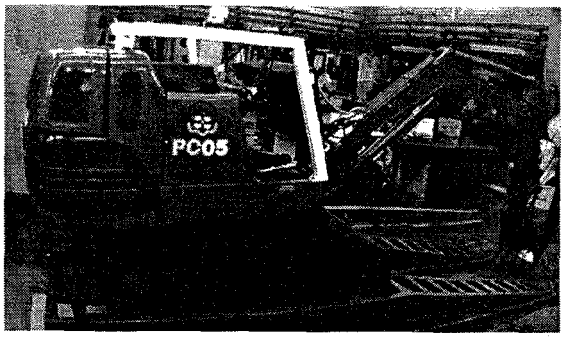

Figure 1: The experimental tracked vehicle

1 Introduction

Real time estimation of soil parameters is essential in achieving precise, robust autonomous guidance and control of a tracked vehicle. Attainment of this objective is important in applications such as mining and earthmoving vehicle automation [1], and of autonomous planetary exploration [2].

The mechanics of tracked vehicles is of continuing interest to organisations and agencies that specify, design and operate tracked vehicles. There is ongoing research activity aimed at extending the feasible operating speed of tracked vehicles, and at refining the accuracy with which a tracked vehicle may be skid steered. Theoretical and experimental work aimed at understanding and controlling the track-soil interaction is being conducted at The University of Sydney. The immediate objective is to allow continuous operation at or near to the manoeuver limit determined by the strength of the soil over which the vehicle is passing. If the nature of the terrain over which the vehicle moves can be identified, estimates of the soil strength can be incorporated into trajectory planning and following algorithms leading to enhanced autonomous or driver-aided operation. That is, given measurements of the vehicle trajectory and the track drive sprocket speeds it is possible to determine key parameters of an assumed soil model. Knowledge of the soil parameters may in turn be used to allow reference trajectories and control algorithms to be adjusted to suit the soil conditions.

A 1.5 tonne tracked vehicle (Fig. 1) has been retrofitted with servo hydraulic actuators and joint force and motion sensors to serve as an experimental platform for this research. The vehicle is also fitted with a wide range of vehicle monitoring and terrain measuring sensors, including INS, GPS, and laser range sensors.

Skid steering a tracked vehicle involves retarding the motion of one track relative to the other to cause the vehicle to turn towards the retarded track. Generally, each track will slip and thus shear the soil in the longitudinal direction. The soil reactions to shearing provide a yawing moment to turn the vehicle, so that the two track drive sprocket angular velocities are the control inputs to the system. The vehicle's motion is determined by the control inputs together with the soil mechanics and the vehicle dynamics. Schiller et al. [3]

give a clear exposition on the nature of this dynamic interaction.

Much of the original work on tracked vehicle mechanics was done by Bekker [4, 5], and is well summarised by Wong [6]. Bekker proposed empirical pressure-sinkage and shear stress-slippage relations based upon extensive experimental data, and provided the basis for later work on the interaction between soil and tracks. Kitano and Kuma [7] modelled the interaction between the tracks and the soil as Coulomb friction, whereas Murakami et al. [8] presented a mathematical model based upon soil plasticity theories for the three dimensional motion of tracked vehicles over soft ground.

Following this introduction, Section 2 presents kinematic and dynamic models of a tracked vehicle undergoing general plane motion. A simple model of the relationship between soil deformation and imposed force is presented. Simulation studies presented in Section 3 demonstrate that an extended Kalman filter (state observer) can be used to estimate track slip from vehicle trajectory data. The method may be extended to allow direct estimation of the soil parameters in real time, providing a basis for precise control of autonomous tracked vehicles.

2 Tracked Vehicle Model

Measurement of the vehicle's trajectory using an inertial navigation system, for example, can provide information on the forces and moments causing the motion. The vehicle's motion plus the angular speed of the track drive sprockets determines the deformation that is imposed on soil elements beneath the tracks. An appropriate soil model then allows determination of the soil-track interaction forces from the imposed deformation. Models of the vehicle dynamics and kinematics, together with a soil model that relates deformation to force are therefore required. The dynamic ("truth") model should have high fidelity, as it will be used to provide truth data in the simulation studies. The soil model will serve as the basis of the estimation algorithms, and need be only sufficiently detailed to capture the significant causal mechanisms relating soil deformation to force.

2.1 Dynamic Model

Figure 2 shows a free body diagram of a tracked vehicle undergoing general plane motion. It is assumed that the centre of mass of the tracks and track frame is located above the centroid of the combined track areas. At the instant shown, the vehicle has velocity components $\dot{x}$, $-\dot{y}$ and $\dot{\Psi}$ in the directions of the vehicle-fixed right-hand frame of reference $f : \{x, y, z, t\}$. As drawn, the vehicle is turning to the left, and may be accelerating in the x, y and Ψ directions. The y-velocity is termed the sideslip velocity, whilst $\dot{\Psi}$ is the yaw rate. The inner and outer tracks develop tractive effort F_i and F_o respectively as a result of shearing the soil in the longitudinal direction. The tracks are also subject to longitudinal resistance forces R_i and R_o that arise as a consequence of the plastic deformation of the soil as the track moves over it. Lateral forces act on the tracks as a consequence of lateral soil shear, and are assumed to be distributed as shown.

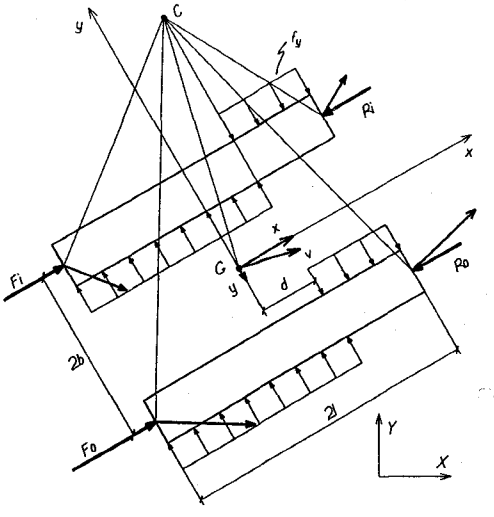

Figure 2: Free body diagram of a tracked vehicle

Also shown in Fig. 2 are the velocities with respect to an inertial frame of reference $F : \{X, Y, Z, t\}$ of several points on the track frame. At the instant shown, the vehicle is moving to the right with a velocity $\dot{x}$, and the track frame is rotating about an instaneous centre C. It can be shown [6] that the instantaneous centre must shift forwards of the track centroid by an amount d [1] that depends on the vehicle's lateral acceleration $\ddot{y}$. This longitudinal shift is required to achieve a nett lateral force to accelerate the vehicle towards the instantaneous centre of rotation, and also reduces the resistive yawing moment. Observe that the vehicle's tracks must be yawed to point *inside* of the velocity vector v_G by an angle α, the slip angle. Observe also that the x-component of track frame velocity must be constant along each track, and that the y component

[1] The notation used here differs slightly from the conventional notation. Here, the track length is $2l$, and the distance between the track centrelines is $2b$. Note that the magnitude of d can exceed l.

of velocity of a point on either track depends only on the longitudinal position of the point, $(x-d)$.

Since the vehicle's centre of mass is above the plane of the track forces, the moment of the centrifugal force during turning will increase the track contact pressure from track front to rear, and from the inside track to the outside track. This effect is neglected for simplicity. It is assumed that the track contact pressure is uniform and constant under both tracks.

For a vehicle of mass m with a moment of inertia I_G about the centre of mass, the equations of motion can be written in the frame f as

$$\begin{aligned} m\ddot{x} &= F_i + F_o - R_i - R_o \\ m\ddot{y} &= 4f_y.d \\ I_G\ddot{\Psi} &= (F_o - R_o)b - (F_i - R_i)b - 2f_y(l^2 - d^2) \end{aligned} \quad (1)$$

where $-l \leqslant d \leqslant +l$. Since the vehicle's motion can be described by $(\dot{\Psi}, \mathbf{v}_G)$, the condition for the y-velocity of the point $(d,0,0)$ in f to vanish leads to the relation $d = \dot{y}/\dot{\Psi}$ which can be used to simplify the equations of motion. It can be seen from the equations that the tractive effort F is available to ovecome the longitudinal resistance R and to accelerate the vehicle. Lateral acceleration can occur only if sideslip is present, and increasing amounts of sideslip diminish the resistive yawing moment provided by the soil.

Equation 1 can be transformed into the frame F as

$$\begin{aligned} m\ddot{X} &= (F_i + F_o - R_i - R_o).cos\Psi - 4f_y.d.sin\Psi \\ m\ddot{Y} &= (F_i + F_o - R_i - R_o).sin\Psi + 4f_y.d.cos\Psi \\ I_G\ddot{\Psi} &= (F_o - R_o)b - (F_i - R_i)b - 2f_y(l^2 - d^2) \end{aligned} \quad (2)$$

2.2 Kinematic Model

A kinematic model of the vehicle that relates the slip parameters to the track frame velocities is required for slip estimation. A suitable model can be written in the frame f and in continuous time as

$$\begin{aligned} \dot{x} &= \frac{r}{2}[\omega_o.(1-i_i) + \omega_i.(1-i_o)] \\ \dot{y} &= -\dot{x}.\tan\alpha = -\dot{x}.\sigma \\ \dot{\Psi} &= \frac{r}{2b}[\omega_o.(1-i_i) - \omega_i.(1-i_o)] \end{aligned} \quad (3)$$

where r is the track rolling radius, $2b$ is the tread of the vehicle, and ω_i and ω_o are the angular speeds of the outside and inside tracks.

The slip parameters are the slip angle coefficient $\sigma = \tan\alpha = -\dot{y}/\dot{x}$ and the inner and outer track slips i_i, i_o

$$i_i = V_{ji}/r.\omega_i, \qquad i_o = V_{jo}/r.\omega_o \quad (4)$$

where V_j is the longitudinal velocity of track sliding with respect to the terrain. The relative sliding velocity depends on the vehicle's motion and the control inputs ω_i and ω_o

$$V_{ji} = \dot{x} - b.\dot{\Psi} - r.\omega_i, \qquad V_{jo} = \dot{x} + b.\dot{\Psi} - r.\omega_o \quad (5)$$

Observe that $r\omega$ is the forward velocity of the track frame in the absence of slip. Slip is defined to be positive when a the tractive effort produced assists the longitudinal motion. Upon transformation into F, the kinematic equations become

$$\begin{aligned} \dot{X} &= \frac{r}{2}[\omega_o.(1-i_i) + \omega_i.(1-i_o)].\cos\Psi + \dot{x}.\sigma.\sin\Psi \\ \dot{Y} &= \frac{r}{2}[\omega_o.(1-i) + \omega.(1-i_o)].\sin\Psi - \dot{x}.\sigma.\cos\Psi \\ \dot{\Psi} &= \frac{r}{2b}[\omega_o.(1-i_i) - \omega_i.(1-i_o)] \end{aligned} \quad (6)$$

2.3 Soil Model

The interaction between soil and a moving track is complicated. The track motion imposes time-dependant normal and shear stresses at the soil surface which are then distributed into the bulk soil via nonlinear stress-strain relationships to produce a complex three-dimensional stress field. Furthermore, the strength of the soil depends on the local normal stress. Although the nature of the interaction has been known for some time [4, 5, 6], numerical techniques such as finite element analysis are required to produce detailed solutions to even static problems. This approach is inappropriate for the present analysis where a relatively simple analytic soil model that captures the essential physics of the track-soil interaction is required to enable real time identification of soil properties

A relatively unsophisticated soil model is adopted here. It is assumed that the soil is homogeneous, and behaves as a rigid-perfectly plastic material. That is, the soil is rigid under increasing loads until a stress condition at which failure occurs is reached, and then undergoes plastic flow. No recoverable elastic deformation occurs.

2.3.1 Tractive Effort

The tractive effort of a track is developed by shearing the terrain, and equals the integral of longitudinal shear stress ove the track contact patch. The maximum tractive effort $F_{\max}$ that can be developed[5] is therefore determined by the contact area A and the shear strength of the terrain $\tau_{\max}$

$$F_{max} = A.\tau_{max} = A.(c + p\tan\phi) \quad (7)$$

Here, p is the normal pressure beneath the track, and the soil parameters are the apparent cohesion c and the angle of internal friction ϕ of the soil. The total tractive effort developed by a track of length $2l$ with a uniform normal pressure distribution can be calculated [6] as a function of the track slip i and the shear deformation modulus, k

$$F = F_{max}.\left[1 - \frac{k}{2l.|i|}(1 - e^{-2l.|i|/k})\right].\text{sign}(i) \quad (8)$$

The form of equation 8 captures the steady-state accumulation of shear deformation from the front to the rear of the track contact patch as a function of track slip $i = V_j/r\omega$ and soil shear stiffness. The shear deformation modulus k is a soil parameter that is related [6] to the surface shear deformation required to cause the soil to fail.

2.3.2 Longitudinal Resistance

Bekker [5] and Wong [6] both use a longitudinal friction coefficient that is independent of velocity, whilst other workers, notably Kar [9], argue that the resistance will depend on velocity. In the present work, it is assumed that the longitudinal resistive force acting on a track is given by

$$R = \mu_x.W \quad (9)$$

where μ_x is effectively a longitudinal friction coefficient, and W is the vehicle weight. This choice is consistant with an assumption of rigid-perfectly plastic soil behaviour with no viscous component and will be a reasonable assumption for operation on well-consolidated mixed or frictional soils. It is perhaps a less sound assumption if the tracked vehicle operates on soft, "sticky" cohesive soils.

2.3.3 Lateral Force and Resistive Moment

Sideslip or yawing motion of the vehicle will cause lateral slippage of track elements, leading to a resistive lateral force and moment. This situation is shown in Fig. 2, which also indicates that a combination of lateral and yaw velocities is equivalent to instantaneous rotation about a point C. Although the functional form of the lateral force per unit length f_y is uncertain, it is clear that points ahead of C in Fig. 2 will be sliding in the positive y direction, whilst those track elements behind C will have a component of sliding velocity in the negative y direction. The relative effect of the lateral forces on the yaw and sideslip motion therefore depends on the distance d. In particular, as the value of d approaches l, maximal lateral acceleration is achieved, but the resistive yawing moment vanishes. A simple model of the lateral resistive force is also adopted here. Following Wong [6] we assume that the lateral force per unit length is

$$f_y = \frac{\mu_y}{2l}.W \quad (10)$$

where μ_y is an effective lateral friction coefficent, and W is the weight force supported by the track.

3 Simulation Results

3.1 Sensitivity of the Vehicle Trajectory to Soil Properties

Figure 3 shows the simulated vehicle trajectories that result from numerically integrating equations 2, 7-10 subject to prescribed control inputs $\omega_i(t)$ and $\omega_o(t)$. Four trajectories are shown: these result from the choice of sets of soil parameters typical of soils of four types, as given in Table 1. Also shown in the figure is the "kinematic" solution that would result in the absence of slip.

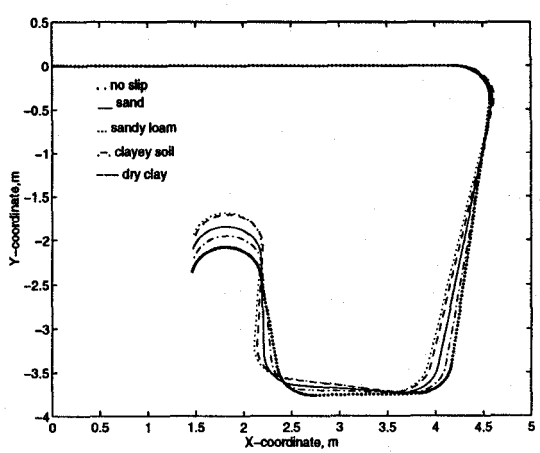

Figure 3: Sensitivity of the vehicle trajectory to soil parameters

Soil Type	c, kPa	ϕ, rad	k, cm	μ_x, -
dry sand	1.04	0.4887	1.0	0.1
sandy loam	1.72	0.5061	2.5	0.1
clayey soil	4.14	0.2269	0.6	0.4
dry clay	68.95	0.5934	0.6	0.2

It is apparant from the figure that the vehicle's trajectory depends to a significant extent on the nature of the soil, particularly when the track drive sprocket speeds command a turn. It follows that measurements of the trajectory can be combined with the command inputs and a suitable soil model to identify the nature of the underlying terrain.

3.2 Identification of Vehicle Slip

Equation 6 is next converted to an equivalent discrete-time state transition equation. A synchronous sampling interval ΔT is assumed, all derivatives are approximated by first-order forward differences, the control inputs $\mathbf{u} = [\omega_i, \omega_o]^T$ are assumed to be approximately constant over the sample period, and all continuous times are replaced with discrete time indices $k \equiv t$, $k+1 \equiv t+\Delta T$. Equation 6 can then be written in the form

$$\mathbf{x}(k) = f(\mathbf{x}(k-1), \mathbf{u}(k)) \qquad (11)$$

The state vector at a time k is $\mathbf{x}(k) = [X(k), Y(k), \Psi(k), i_i(k), i_o(k), \sigma(k)]^T$, the control vector is $\mathbf{u}(k) = [\omega_o(k), \omega_i(k)]^T$ and the nominal state transition equation is given by 11. It is clear from equation 6 that the state-transition equation is nonlinear, so that the extended Kalman filter [10] is required for estimation. Process and observation models

$$\mathbf{x}(k) = f(\mathbf{x}(k-1), \mathbf{u}(k)) + \mathbf{v}(k) \qquad (12)$$
$$\mathbf{z}(k) = \mathbf{H}(k).\mathbf{x}(k) + \mathbf{w}(k) \qquad (13)$$

are assumed, where $\mathbf{v}(k)$ is the process noise, $\mathbf{z}(k) = [X_{obs}, Y_{obs}, \Psi_{obs}]^T$ is the observation and $\mathbf{w}(k)$ is the observation noise.

The extended Kalman filter (EKF) was used to estimate the track slip parameters during simulated motion of the experimental tracked vehicle when manoeuvering on different soils. During the motion the EKF receives the control inputs ω_o, ω_i and the position (X, Y, Ψ) from the truth model as observations. The EKF then estimates the position of the vehicle, and computes the slips i_o and i_i of both tracks, and the slip angle α. It can be seen from figures 4 to figure 8 that the EKF performance is good. The true trajectory is followed closely, and the track slip is estimated by the filter with a reasonably small time lag.

The figures 4 and 5 compare the observed and estimated slips of both tracks and the slip angle on sandy loam and dry clay. As the slips on sandy loam are significant when the vehicle is turning, the filter can detect and estimate them relatively accurately. On

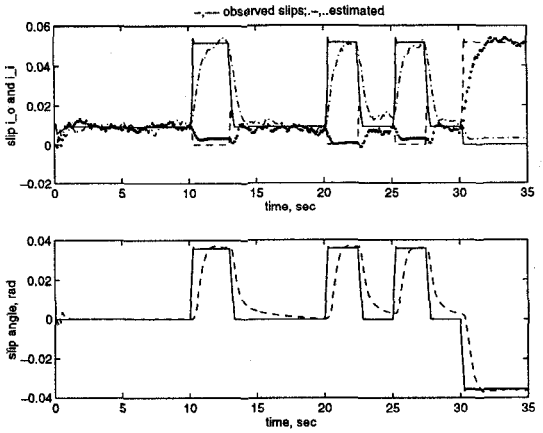

Figure 4: Track slip when moving on sandy loam

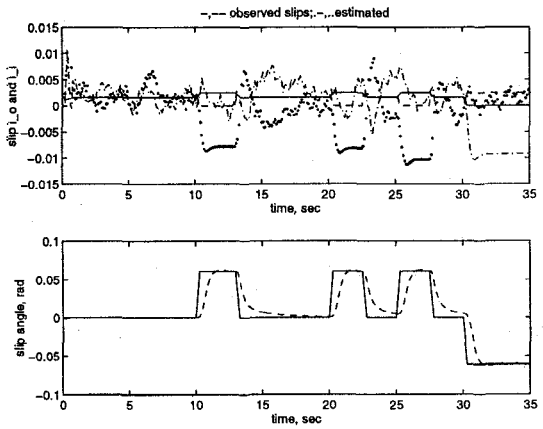

Figure 5: Track slip when moving on dry clay

dry clay the slips are small, about 1%. It is therefore harder to distinguish them from the observation and process errors, although the filter still can determine when the vehicle is turning. Figure 6 show the position estimation errors, which are clearly within the two standard deviations (dashed line) of the mean error. The esimation error and innovation in heading angle are shown in Figures 7 and 8. These figures show that the state observer tracks the heading angle over straight motion segments, but fails to track when the vehicle turns abruptly. Further optimisation of the filter is required to compensate for this behaviour.

4 Conclusions and Future Work

The simulation results presented in the previous section show that it is possible to estimate the slip of a tracked vehicle from trajectory measurements. Once

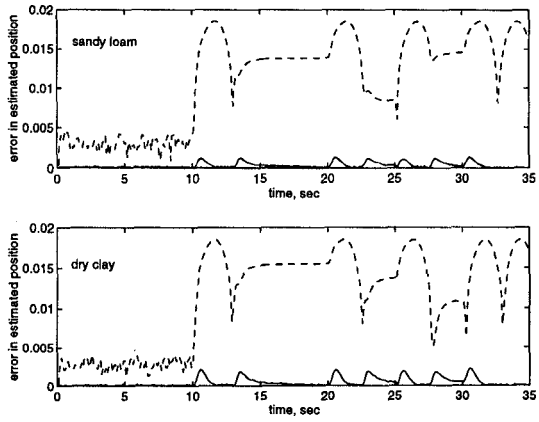

Figure 6: Error in estimated position when moving on sandy loam and dry clay

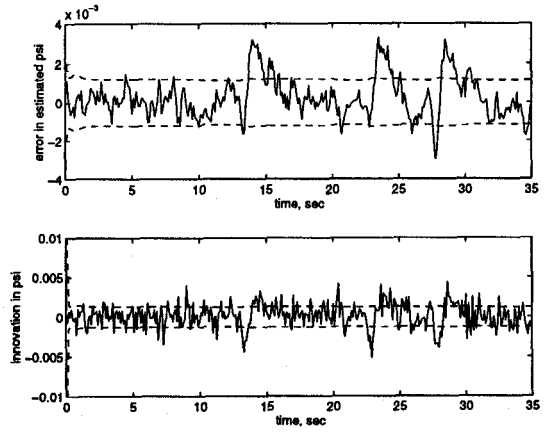

Figure 7: Error in estimation of heading angle Ψ, and innovation in Ψ when moving on sandy loam

estimates of the slip are obtained, these can be combined with the soil model and estimates of the tractive effort in another nonlinear estimation structure to give estimates of the soil parameters. Knowledge of the soil properties will allow intelligent autonomous control of a tracked vehicle through modification of the vehicle trajectory or trajectory-following algorithms in real time. In addition to this theoretical extension, there is considerable work directed at experimentaly testing the theory using the experimental vehicle.

5 Acknowledgement

The writers wish to acknowledge the assistance of NS Komatsu Pty. Ltd, who donated the Komatsu PC05 mini excavator.

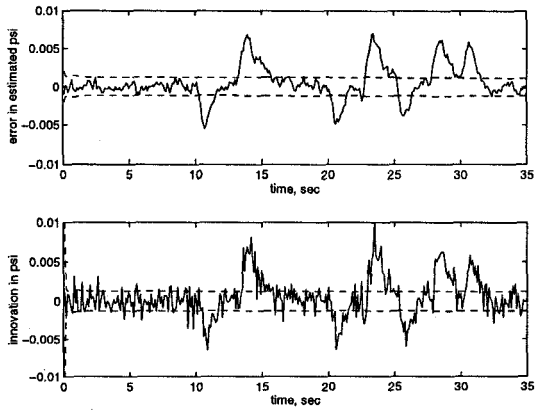

Figure 8: Error in estimation of heading angle Ψ, and innovation in Ψ when moving on dry clay

References

[1] R.H. King. "State-of-the-art in mine automation", in *Proc 87th Ann. Meeting*, Rocky Mountain Coal Mining Inst., Keystone, CO, 1991.

[2] P.J.A. Lever and F-Y Wang. "Intelligent excavator control system for lunar mining system", *J. Aerospace Engineering*, vol. 8, no. 1, pp. 16-24.

[3] Z. Shiller, W. Serate and M. Hua. "Trajectory planing of tracked vehicles," *IEEE Trans. Robotics and Automation*, vol. 3, pp. 796 - 801, 1993.

[4] M. G. Bekker. *Theory of Land Locomotion.* Ann Arbor: University of Michigan Press, 1962.

[5] M. G. Bekker. *Introduction to Terrain–Vehicle Systems.* Ann Arbor: University of Michigan Press, 1969.

[6] J. Y. Wong. *Theory of Ground Vehicles.* New York: Wiley, 2. ed., 1993.

[7] M. Kitano and M. Kuma. "An analysis of horizontal plane motion of tracked vehicles," *J. Terramechanics*, vol. 14, pp. 211 - 225, 1977.

[8] H. Murakami, K. Watanabe and M. Kitano. "A mathematical model for spatial motion of tracked vehicles on soft ground," *J. Terramechanics*, vol. 29, no. 1, pp. 71 - 81, 1992.

[9] M. K. Kar. "Prediction of track forces in skid-steering of military tracked vehicles," *J. Terramechanics*, vol. 24, no. 1, pp. 75 - 86, 1987.

[10] H. F. Durrant–Whyte. "An autonomous guided vehicle for cargo handling applications", *I. J. Robotics Research*, vol. 15, no. 4, 1996.